

## Measurement of Neutron Flux at the NSCL K1200 Cyclotron for 80 MeV/u $^{18}\text{O}^{6+}$ Beam on a $^9\text{Be}$ Target

SALEM ALI SALEM SHAHEEN\*

*Department of Physics, Faculty of Science,  
King Abdulaziz University, Jeddah, Saudi Arabia*

**ABSTRACT.** The neutron flux at the NSCL K1200 cyclotron accelerator target at the National Superconducting Cyclotron Laboratory (NSCL), East Lansing, MI, USA, was measured by using the foil activation method. Several  $^{115}\text{In}$  and  $^{27}\text{Al}$  foils were irradiated at different positions around the target. The induced activities were counted by the HPGe detector and a personal computer multi-channel analyzer. Angular distributions of the flux are presented. The data are compared with those in the literature.

### Introduction

When an energetic beam hits a target, different types of radiation such as gammas and neutrons come out with different energies as a result of the fragmentation or break-up process<sup>[1]</sup>. The neutron fluxes from such reactions are large. Tuyn *et al.* used a current of the order of  $10^{11}$   $^{12}\text{C}$  ions per second at 86 MeV/u on an iron target with  $^{115}\text{In}$ ,  $^{32}\text{S}$ ,  $^{27}\text{Al}$  and  $^{12}\text{C}$  as activation detectors to measure the neutron fluxes<sup>[2]</sup>. They reported fast neutron (< 20 MeV) flux of  $5 \times 10^9$  n.cm<sup>2</sup>/g.s.sr (normalized to the target thickness and solid angle) using  $^{27}\text{Al}$  foil at 100 cm from 3.2 g/cm<sup>2</sup> Fe target, at 0°. It is expected that the neutron flux will increase using heavier and more neutron-rich beams. This is displayed in this experiment with a current of  $7.3 \times 10^{11}$   $^{18}\text{O}^{6+}$  ions per second at 80 MeV/u on a 1.9 g/cm<sup>2</sup>  $^9\text{Be}$  target with  $^{27}\text{Al}$  as activation detector too.

Activation foils are used for flux measurements because they are known for their reliability and convenience<sup>[3,4]</sup>. Unlike some detectors, activation foils need no electronics during the irradiation nor do they get disabled by high fluxes. There is no interference from other radiation, like gamma-rays. The foils respond only to neutrons, therefore neutron-induced gamma activity can be conveniently counted by a simple set-up with a high resolution detector, like a high-purity germanium (HPGe) detector, and a multichannel analyzer.

\*This experiment was done in 1997 during a sabbatical leave at NSCL, USA.

## Experimental Setup and Method

### 1. Activation Foils

In this experiment, neutrons were detected by twelve activation foils. These foils were divided into three groups, A, B and C as seen in Fig. 1a. Groups B and C have an aluminum foil and two indium foils, (see Table 1). In each group, one of the indium foils was covered with cadmium foils on both sides to absorb the thermal neutrons. Group A has six foils, five of them are put on the outside surface of a 16.5 cm × 16.5 cm cylindrical neutron moderator. These foils are an aluminum foil, two bare indium foils and two indium foils covered with cadmium foils on both sides. The sixth is an indium foil which was placed inside the moderator at its center (see Fig. 1a).

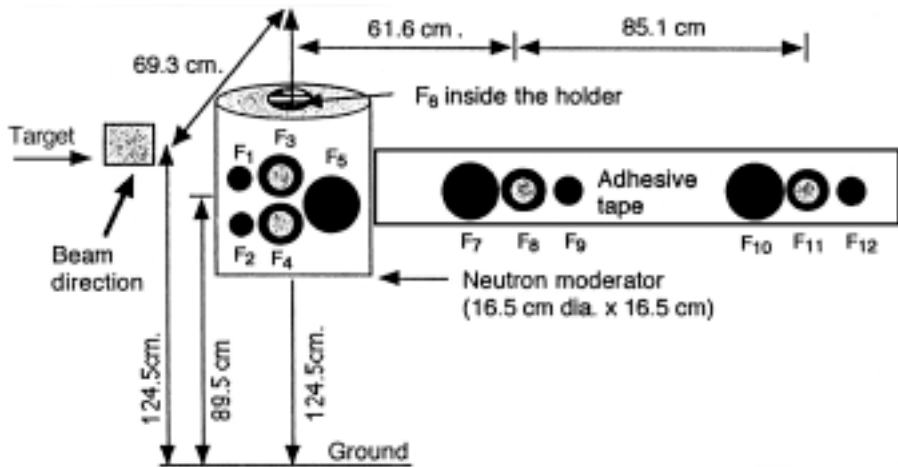


Fig. 1a. A front view of the experimental setup where foils 1-12 were irradiated (not to scale). Foils 1-5 were placed on the outside surface of the moderator under the beam line and facing the beam direction. Foil 6 was put inside the moderator at the center. Foils 7-12 were placed on an adhesive cloth tape.

TABLE 1a. The different activation foils used in the experiment.

| Element of the foil | Foil number                             | Average mass (g)     | Average diameter (cm) | Average thickness (cm) | Purity % |
|---------------------|---|----------------------|-----------------------|------------------------|----------|
| $^{115}\text{In}$   | 1, 2, 3, 4, 6, 9, 12<br>3*, 4*, 8*, 11* | $0.9192 \pm 0.0112$  | $2.5400 \pm 0.0500$   | $0.0248 \pm 0.0003$    | 99.9959  |
| $^{27}\text{Al}$ ** | 5, 7, 10                                | $14.1340 \pm 0.5688$ | 5.1                   | $0.2650 \pm 0.0093$    | 99.00    |

\*These are covered by cadmium foils on both sides.

\*\*Aluminum foils were cut out from the same rod.

The location of each group relative to the other groups, the cyclotron target and the beam line is seen in Fig. 1. All the groups were placed at positions approximately 34.9 cm lower than the plane of the target and beam line such that they faced the beam. Group A was located under the beam line while groups B and C were put on an adhesive cloth tape, Fig. 1a. The distances from the target to groups locations, distances among the

groups and the angular separations relative to the beam line (taken as  $0^\circ$ ) are explained in Table 1 and Fig. 1. As seen all the groups are in the forward direction.

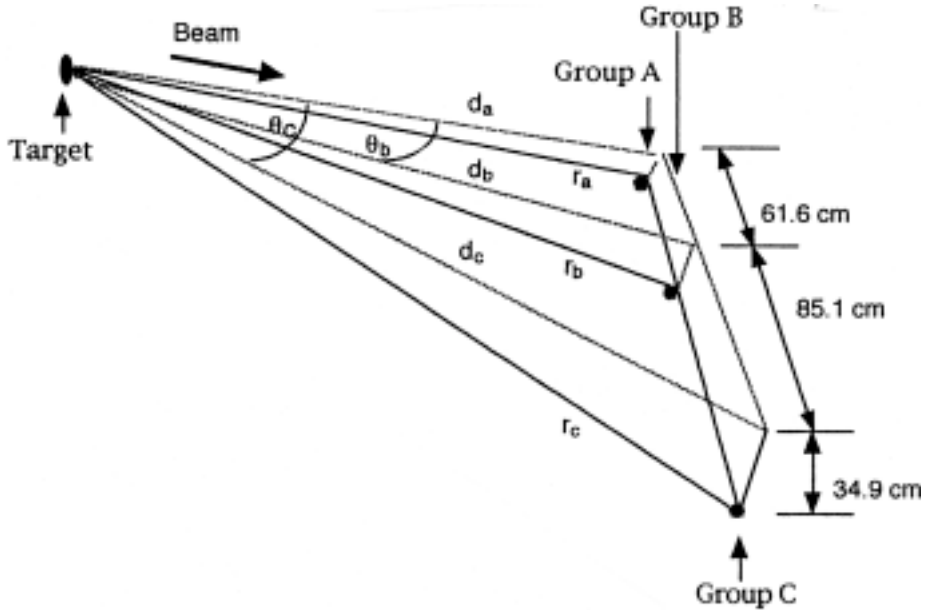


Fig. 1b. A side view of the experimental setup (see Table 1). The lines  $d_a$ ,  $d_b$ ,  $d_c$ , the beam line and target are in plane that makes an angle of  $26.8^\circ$  with a lower plane of the lines  $r_a$ ,  $r_b$  and  $r_c$ . The vertical distance, between the upper plane and the position of the groups line is 34.9 cm.

TABLE 1b. The three groups of foils and their approximate angles and distances from the target.

| Group | Foils in the group                 | Distance* from the target, $d$ (cm) in the upper plane | Distance* from the target, $r$ (cm) in the lower plane | The angle of each group relative to the beam line |
|-------|------------------------------------|--|--|---|
| A     | $F_1, F_2, F_3$<br>$F_4, F_5, F_6$ | 69.25**  | 77.56**  | $\theta_a = 0^\circ$                              |
| B     | $F_7, F_8, F_9$                    | 92.68  | 99.04  | $\theta_b = 41.7^\circ$                           |
| C     | $F_{10}, F_{11}, F_{12}$           | 162.21   | 165.93   | $\theta_c = 64.7^\circ$                           |

\*Measurements were made to the center of the group.

\*\*These distances are measured to the center of the moderator where  $F_6$  is located. The rest foils of the group are 8.25 cm closer to the target on  $d$ .

The average masses, diameters, thicknesses and the purities are given in Table 1a. For cadmium cover foils the values are  $3.20 \pm 0.23$  g, 3 cm and  $0.052 \pm 0.004$  cm respectively.

## 2. Irradiation of the Foils

The irradiation time of the foils at the locations described above is approximately 67 hours. The possible reactions are  $^{115}\text{In}(n_{\text{th}} \text{ or } n_{\text{ep}}, \gamma)^{116\text{m}}\text{In}$  and  $^{27}\text{Al}(n_{\text{f}}, \alpha)^{24}\text{Na}$  where  $n_{\text{th}}$  is a thermal neutron,  $n_{\text{ep}}$  is an epithermal neutron and  $n_{\text{f}}$  is a fast neutron. The ab-

sorption cross-section for  $n_{th}$  is  $170 \pm 15$  b at 0.025 eV and for  $n_{ep}$  is  $3243 \pm 35$  b at a resonance energy of 1.457 eV. The threshold for the second reaction is 7.2 MeV with the absorption cross-section of  $0.693 \pm 0.045$  mb<sup>[3,5]</sup>. The irradiation time when compared with the half lives of the product nuclei (for  $^{116m}In$ ,  $T_{1/2} = 54.4$  minutes and for  $^{24}Na$ ,  $T_{1/2} = 15$  hours) is long enough for In foils to reach 100% of the saturation activity and Al foils 95.5% of saturation. This can be concluded from the relation<sup>[6]</sup>

$$A = A_{sat.} (1 - e^{-\lambda t}) \quad (1)$$

where  $A_{sat.}$  is the saturation activity. Since the integrated flux of the incident neutrons over the irradiation period is proportional to the induced activity in the foils<sup>[4]</sup>, it becomes important to know the saturation fraction of the foil which leads to the number of the excited nuclei.

The beam from the K1200 cyclotron is  $^{18}O^{6+}$  on a  $1.9 \text{ g/cm}^2$   $^9Be$  target with beam current is 700 ena (electron nanoampere) at 80 MeV/u or, therefore  $7.3 \times 10^{11}$  ions/s.

### 3. Counting the Foils.

Each foil was counted for 10 minutes (with an average dead time less than 2% for Al foils, about 24% for bare In foils and about 12% for the rest of the In foils), by an energy calibrated 75.5 mm (diameter)  $\times$  92.0 mm (long) hyperpure germanium (HPGe) detector that has an active volume of  $411.67 \text{ cm}^3$ . Each foil was counted at 5 cm from the center of the front face of the detector crystal. This counting position and the detector were well shielded by lead bricks. All foils were counted within 3 hours after the end of the irradiation.

Several gamma standard sources ( $^{60}Co$ ,  $^{22}Na$ ,  $^{133}Ba$ ,  $^{54}Mn$ ,  $^{57}Co$ ,  $^{109}Cd$ ) were used for full-energy peak efficiency (Fig. 2) and energy calibration of the HPGe detector. The activity of these standard sources ranges from 1-12  $\mu Ci$ . The latter had a FWHM energy resolution of 4.5 keV at 1332.5 keV of  $^{60}Co$ . Although the resolution should be better than this, the gamma peaks were well resolved as can be seen in Fig. 3. The same geometrical position relative to the HPGe detector was preserved during the different stages of the work. The absolute full-energy peak efficiency was corrected for the coincidence summing effect in the case of  $^{60}Co$ ,  $^{22}Na$  and  $^{133}Ba$  which are multiple-line  $\gamma$  sources, thus coincidence correction is relevant. On the other hand,  $^{54}Mn$ ,  $^{57}Co$  and  $^{109}Cd$  are single-line  $\gamma$  sources and don't require this correction<sup>[7]</sup>. Since summing effects depend on the square of the detector solid angle<sup>[8]</sup>, the summing correction factors for this detector were calculated by scaling from correction factors of another HPGe detector with the same geometrical positions but a 1 and 10 cm from the detector<sup>[9]</sup>. The dead time during the efficiency measurement is less than 2%. The experimental efficiency data points, Fig. 2, were fitted by the equation.

$$\epsilon = a + b (E)^{0.5} \ln E + c \ln(E) / E^2 + d/E^2 \quad (2)$$

where  $\epsilon$  is the efficiency. The constants  $a = 1752.21 \times 10^{-3}$ ,  $b = -3386 \times 10^{-6}$ ,  $c = 4941 \times 10^{-1}$  and  $d = -2161.5096 \times 10^{-2}$  are the fitting parameters. The fit goodness parameter  $\kappa^2$  is 0.998. The uncertainty of about 3.1% in the experimental efficiency data points is due to the counting statistics.

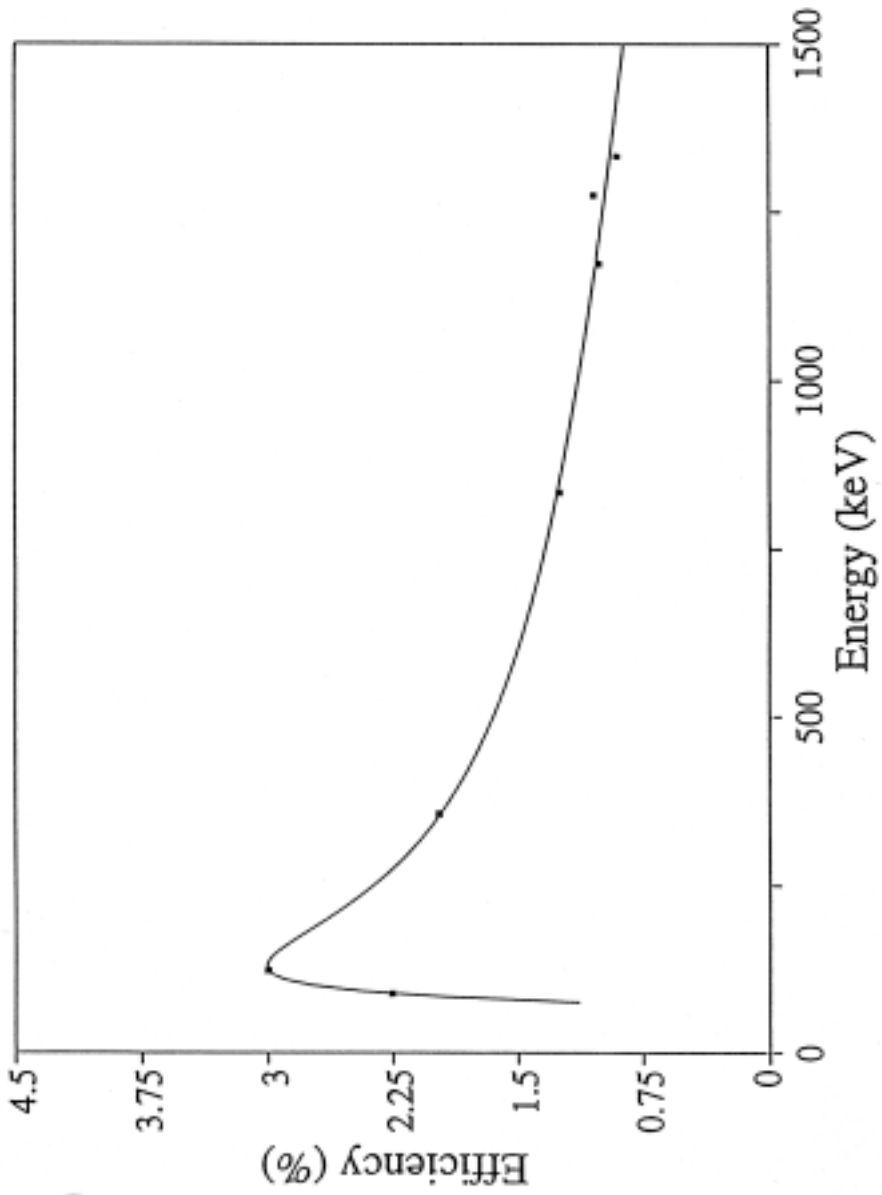


FIG. 2. The efficiency curve of the hyper pure germanium detector used in this experiment. Data points were fitted by the curve.

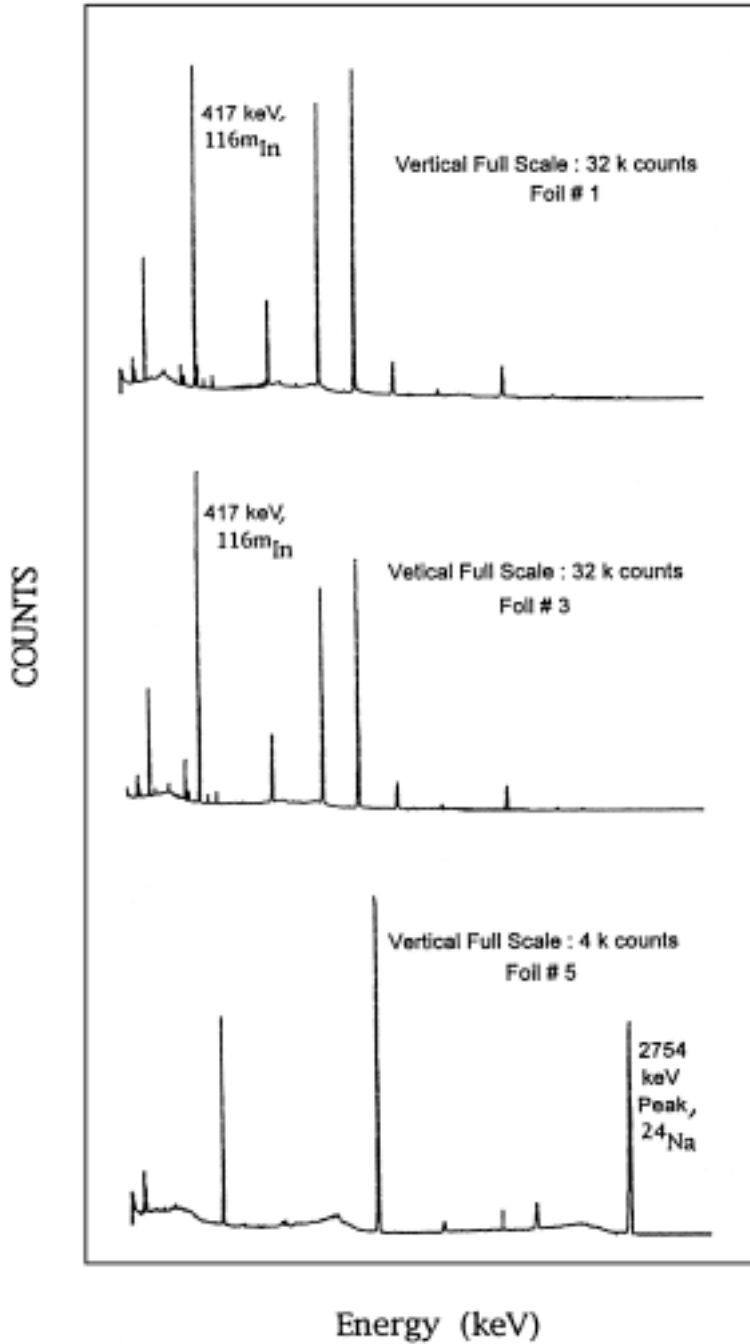


Fig. 3. The gamma ray spectra from counting: (top) the bare  $^{115}\text{In}$  foil  $F_1$ , (middle) the cadmium covered  $^{115}\text{In}$  foil  $F_3$  and (bottom) the  $^{27}\text{Al}$  foil,  $F_5$ .

### Analysis and Results

Both slow or thermal ( $E_n < 0.5$  eV) and intermediate or epithermal ( $0.5$  eV  $< E_n < 10$  keV) absorption activations follows (n,  $\gamma$ ) reaction<sup>[3]</sup>.  $^{115}\text{In}$  has a large neutron absorption cross-sections in the thermal and epithermal energy ranges and can be used as neutron detector for these energies. The product nucleus of the above reaction is  $^{116\text{m}}\text{In}$  which decays by emitting several gamma lines. One of these lines, the 417 keV line with absolute intensity of 32.4%, was observed in this experiment and used for flux calculations. Unlike the thermal and epithermal neutrons, fast neutrons ( $E_n > 10$  keV) are detected by threshold activation in which a nuclear particle is emitted such as (n, p), (n, n) and (n,  $\alpha$ ) reactions. In this experiment  $^{27}\text{Al}$  foil was used to identify fast neutrons through the  $^{27}\text{Al}$  (n,  $\alpha$ )  $^{24}\text{Na}$  reaction.  $^{24}\text{Na}$  decays by emitting  $\beta^-$  particle with 100% to two excited states of  $^{24}\text{Mg}$  which decays to its ground state by emitting the two  $\gamma$ -lines 1368 and 2754 keV. In this experiment, the induced activity of the 2754 keV line (net area of the peak) was used for fast neutron flux calculation whereas the induced activity of the 417 keV line in the Cd covered  $^{115}\text{In}$  foil was used for the intermediate energy fast neutron flux. By subtracting the counts of the 417 keV line in the Cd- covered  $^{115}\text{In}$  foil which was used for intermediate fast neutron flux from the counts of the 417 keV line in the bare.  $^{115}\text{In}$ , thermal neutrons counts are determined<sup>[3]</sup>. This was done because bare  $^{115}\text{In}$  detects both thermal and epithermal neutrons with the same reaction. These counts were corrected for background. The flux is calculated by the following equation<sup>[3]</sup>:

$$\Phi = \Delta N / [\sigma(1E-24) N_s \text{SAPEB} (\text{exp.} - \mu_s (X_s/2)) (\text{exp.} - \mu_a X_a) (\text{exp.} - \sum_n X_s) (\text{exp.} - \lambda t_d) (1 - (\text{exp.} - \lambda t_i)) (1 - (\text{exp.} - \lambda t_c))] \quad (3)$$

where

- $\Phi$  = neutron flux (n/cm<sup>2</sup>.s)
- $\Delta N$  = number of counts during the counting time  $t_c$  in seconds.
- $\sigma$  = cross section (barn).
- $N_s$  = number of nuclei in the foils ( $^{115}\text{In}$ ,  $^{27}\text{Al}$ ).
- $S$  = saturation fraction of the foil.
- $A$  = abundance fraction of foil.
- $P$  = purity fraction of the foil.
- $E$  = efficiency of the detector (HPGe) at the relevant energies of gamma.
- $B$  = the absolute intensity of gamma line of interest.
- $\mu_s(X_s/2)$  = the total attenuation coefficient of gamma in the foils with  $\mu_s$  at the relevant energies and the half thickness of the foil  $X_s/2$ .
- $\mu_a X_a$  = the total attenuation coefficient of gamma in air  $\mu_a$  at the relevant energies and the separation between the foils and the detector  $X_a$ .
- $\sum_n X_s$  = the attenuation of neutrons in the foils  $\sum_n$  at the relevant energies and foil thickness ( $X_s$ ).
- $t_i, t_d, t_c$  = irradiation, decay and counting periods were the counting time was corrected for the dead time. The decay time was taken from the end of irradiation to the midpoint of the counting interval.
- $\lambda$  = decay constant for the product nuclei ( $^{116\text{m}}\text{In}$  and  $^{27}\text{Al}$ ).

The flux results are listed in Table 2. It should be noticed that the flux values calculated for A, B and C groups at 1 cm from the target have approximately the same order of magnitude and they average to  $3.6 \times 10^{11}$  n/cm<sup>2</sup>.s for thermal,  $4.3 \times 10^{10}$  n/cm<sup>2</sup>.s for intermediate and  $2.9 \times 10^{15}$  n/cm<sup>2</sup>.s for fast. The uncertainty in these values is about 9.4% for thermal, 3.4% for intermediate and 7.7% for fast neutrons. This uncertainty is due to counting statistics, cross-sections and efficiency. Since the induced activity (of 2754 keV <sup>24</sup>Na peak here) is proportional to the fast neutron flux with energies above the threshold<sup>[3]</sup>, this flux was calculated using the cross-section of 0.693 mb at the threshold of 7.2 MeV. It is not known from what depth in the foil  $\gamma$ -ray was emitted, therefore half the foil thickness was used to correct for the self absorption. However, this correction is only about 2.5% which is smaller than the uncertainty in the flux values. The correction for neutron attenuation in <sup>115</sup>In was neglected because neutrons will be absorbed in these foils due to their low energy. In addition to that, the thickness of <sup>115</sup>In foils is very small (see Table 1a). This wasn't the case of the relatively thicker <sup>27</sup>Al foils which interact with fast neutrons.

TABLE 2. The neutron fluxes at the different locations in this experiment\*.

| Group |   | Neutron energy                  | At the sample position     | At 1 cm from target position** |
|-------|---|---------------------------------|----------------------------|--------------------------------|
| A     | Flux (Neutrons / cm <sup>2</sup> .s)                  | Thermal<br>Intermediate<br>Fast | 5.9E8<br>7.4E7<br>1.4E13   | 2.3E11<br>2.9E10<br>5.4E15     |
|       | $\frac{\text{Neutrons / cm}^2}{\text{Beam particle}}$ | Thermal<br>Intermediate<br>Fast | 8.1E-4<br>1.0E-4<br>1.9E1  | 3.2E-1<br>4.0E-2<br>7.4E3      |
| B     | Flux (Neutrons / cm <sup>2</sup> .s)                  | Thermal<br>Intermediate<br>Fast | 3.3E8<br>4.0E7<br>2.9E12   | 2.6E11<br>3.1E10<br>2.3E15     |
|       | $\frac{\text{Neutrons / cm}^2}{\text{Beam Particle}}$ | Thermal<br>Intermediate<br>Fast | 1.5E-4<br>5.4E-5<br>4.0E0  | 1.2E-1<br>4.3E-2<br>3.1E3      |
| C     | Flux (Neutrons / cm <sup>2</sup> .s)                  | Thermal<br>Intermediate<br>fast | 2.7E8<br>3.2E7<br>4.9E11   | 6.0E11<br>7.1E10<br>1.1E15     |
|       | $\frac{\text{Neutrons / cm}^2}{\text{Beam particle}}$ | Thermal<br>Intermediate<br>Fast | 3.8E-4<br>4.4E-5<br>6.8E-1 | 8.3E-1<br>9.7E-2<br>1.5E3      |

\*80 MeV/u <sup>18</sup>O<sup>6+</sup> beam on an 1.9 g/cm<sup>2</sup><sup>9</sup>Be target.

\*\*These values are calculated from the measured values at the sample position.

Being inside a neutron moderator, F<sub>6</sub> (<sup>115</sup>In foil) detected thermalized fast neutrons. The energy response of the moderator is essentially uniform from 20 keV to 20 MeV<sup>[4]</sup>. The fast flux at 1 cm from the target position measured by F<sub>6</sub> is  $1.9153 \times 10^{11}$  n/cm<sup>2</sup>.s. This is very much less than the other value of the same neutron group which was measured by <sup>27</sup>Al foil, F<sub>5</sub>. This can be justified by considering the difference of the reactions in the



two cases. The reaction in  $^{27}\text{Al}$  is insensitive for neutrons with  $E_n < 7.2$  MeV whereas  $F_6$  is very sensitive to all fast neutrons that were thermalized by the moderator.  $F_6$  is also about 7 cm farther from the target and was located behind all the foils which were positioned on the moderator surface. This may led to degrading the flux at the  $F_6$  location.

The angular distribution a of the flux at the same radial distance of 70.32 cm from the target is presented in Fig. 4. It should be noticed that the flux values for each type of neutron differ by a factor of 10 at the most.

### Conclusion

The data and the results of this experiment show that the neutron flux measured in this experiment correspond to a flux of about of  $10^{11}$  n/cm<sup>2</sup>.s for thermal neutrons,  $10^{10}$  n/cm<sup>2</sup>.s for intermediate energy neutrons and  $10^{15}$  n/cm<sup>2</sup>.s for fast neutrons at 1 cm from the target. The 0° fast neutron flux calculated at 100 cm and normalized to 1.9 g/cm<sup>2</sup>  $^9\text{Be}$  target thickness is  $3.6 \times 10^{16}$  n.cm<sup>2</sup>/g.s.sr, which is much higher than Tuyn's value of  $5 \times 10^9$  n.cm<sup>2</sup>/g.s.sr<sup>[2]</sup>. This experiment was done at comparable beam intensity and energy per beam ion, to those of Tuyn *et al.* Therefore this difference can be justified, in part, by the heavier, more neutron-rich beam that was used in this experiment. Also, different cross-sections  $\sigma(n_f \text{ on } ^{27}\text{Al})$  were used. Tuyn *et al.* used  $\sigma(n_f \text{ on } ^{27}\text{Al})$  of 63 mb which is about  $10^2$  larger than  $\sigma(n_f \text{ on } ^{27}\text{Al})$  of 0.693 mb used in this experiment. Using  $\sigma(n_f \text{ on } ^{27}\text{Al})$  of 63 mb, the flux will be  $4 \times 10^{14}$  n.cm<sup>2</sup>/g.s.sr.

Due to the induced activities in near by objects such shielding walls, vacuum chambers and slits when struck by the beam, neutron flux and any other secondary radiation ( $\alpha$ ,  $\beta$  and  $\gamma$ ), this data is relevance to laboratories for the safety of workers and experiment electronics<sup>[10]</sup>. Depending on the half lives of the different elements formed, the induced activities may last for many hours or days after the shut down of the beam.

The application of the foil activation detection system reflects their simplicity and practicality. This suggests that these types of measurements should be done more frequently during the laboratory approved experiments using different beams and setups.

### References

- [1] Charvet, J.L., Duchene, G., Joly, S., Magnago, C., Morjean, M., Patin, Y., Pranal, Y., Sinopoli, L., Uzureau, J.L., Billerey, R., Chambon, B., Chbihi, A., Chevarier, A., Chevarier, N., Drain, D., Pastor, C., Stern, M., Peghaire, A., *Physics Letters B*, **189**(4): 388 (1987).
- [2] Tuyn, J.W.N., Deltenre, C., Lamberet, C. and Roubaud, G., *Proc. 6th Int. Cong. IRPA, Berlin*, 673 (1984).
- [3] Scientific Staff, *Activation Foil Manual*, Reactor Experiment Inc., California, USA (1965).
- [4] Scientific Staff, *Neutron Flux Integrator*, Reactor Experiment Inc., California, USA (1965).
- [5] Erdtmann, G., *The Neutron Activation Tables*, vol. 6, Verlag-Chemie, New York (1976).
- [6] Lamarsh, J.R., *Introduction to Nuclear Engineering*, Addison-Wesley, third edition (1977).
- [7] Quittner, P., *Gamma-Ray Spectroscopy*, second edition, Hilger, p. 98 (1973).
- [8] Ramos-Lerate, I., Barrera, M., Ligeró, R.A. and Casas-Ruiz, M., *Nuclear Instruments and Methods*, **A395**: 202 (1997).
- [9] Aksoy, A., *Journal of Radioanalytical and Nuclear Chemistry*, **169**(2): 463 (1993).
- [10] **Radiation Safety Manual**, National Superconducting Cyclotron Laboratory, East Lansing, Michigan, USA (1996).

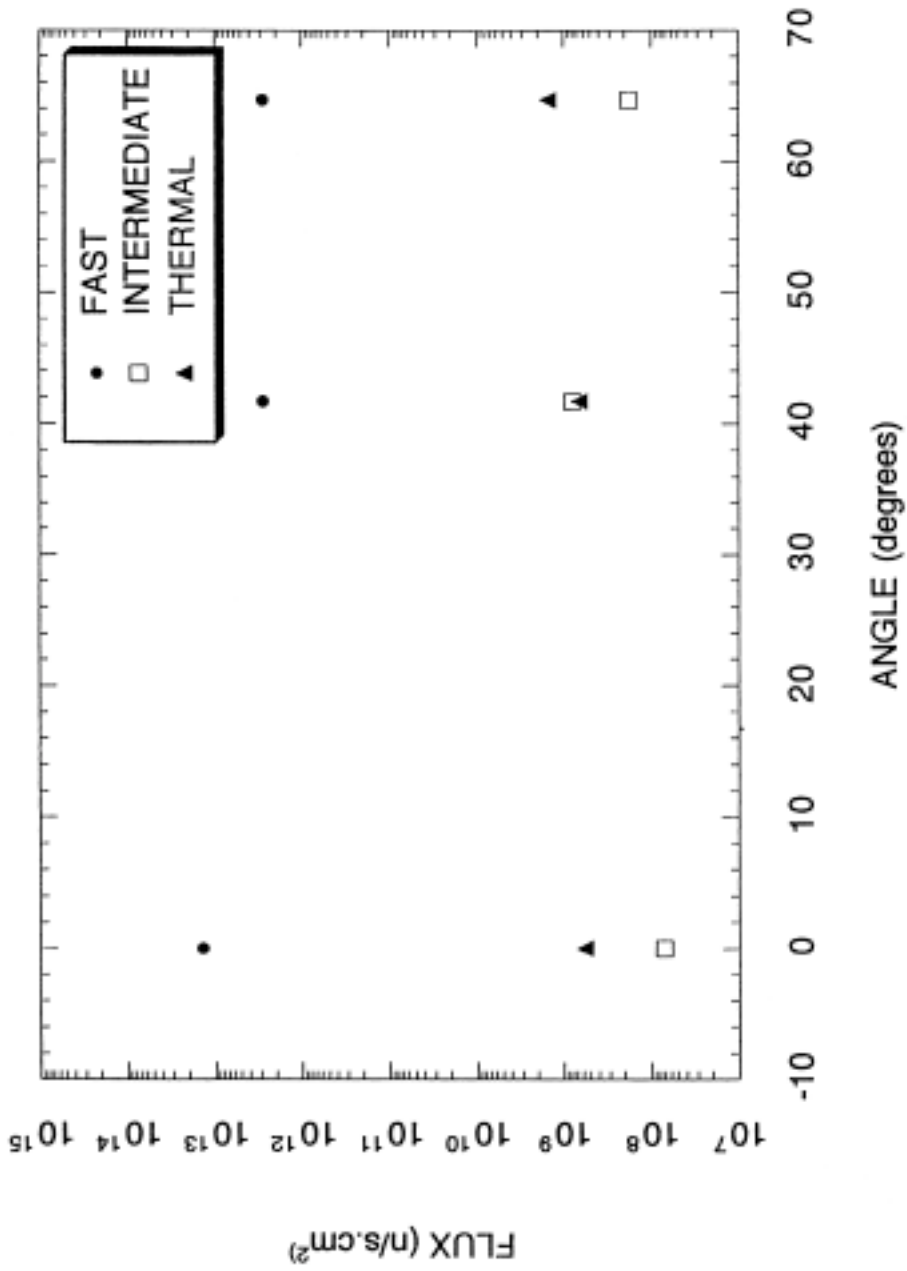


FIG. 4. The angular distribution of the flux at the foil locations for the thermal, intermediate and fast neutrons.

قياس الفيض النيوتروني في المعمل الوطني للمعجل الدائري فائق  
التوصيل K1200 باستخدام التفاعل النووي لشعاع أيوني من  
 $^{18}\text{O}^{+6}$  معجل بطاقة قدرها ٨٠ ميغا إلكترون فولت لوحد الكتلة  
الذرية ، مع الهدف  $^9\text{Be}$

سالم علي سالم شاهين  
قسم الفيزياء ، كلية العلوم ، جامعة الملك عبد العزيز  
جدة - المملكة العربية السعودية

المستخلص . تم قياس الفيض النيوتروني قريباً من هدف المعجل الدائري فائق التوصيل K1200 في المعمل الوطني بمدينة ايست لانسنج بولاية ميشيجان في الولايا المتحدة الأمريكية باستخدام التنشيط الاشعاعي لعدد من صفائح  $^{115}\text{In}$  و  $^{27}\text{Al}$  وضعت في مواقع متعددة حول هدف المعجل . ولقد حسب النشاط الاشعاعي الناتج عن التشعيع باستخدام كاشف جرمانيوم بالغ النقاوة ، وحاسب شخصي يحوي محلل متعدد القنوات . كما يعرض التوزيع الزاوي للفيض ومقارنة نتائج هذا البحث بنتائج أبحاث أخرى .